

Shape of the β spectra in the $A = 14$ system

A. García

Department of Physics, University of Notre Dame, Notre Dame, Indiana 46556

B.A. Brown

National Superconducting Cyclotron Laboratory, Department of Physics and Astronomy, Michigan State University, East Lansing, Michigan 48824-1321

(Received 8 June 1995)

We calculate the shape of the β^- and β^+ spectra in the $A = 14$ system using constraints from measurements of the width of the $M1$ transition, $^{14}\text{N}(e, e')$ cross section, and $\log ft$ values, as well as shell-model wave functions. Our result for the shape factor assuming conservation of vector current disagrees by a factor of 2 with existing data from ^{14}O β^+ decay.

PACS number(s): 23.40.Hc, 21.60.Cs, 24.80.Dc, 27.20.+n

I. INTRODUCTION

The energy dependence of allowed β spectra is given by [1,2]

$$dN/dW_e = \frac{G_\beta'^2}{2\pi^3} [A_0^2 + C_0^2] F_0 L_0 C(W_e) p_e W_e (W_0 - W_e)^2 \quad (1)$$

where W_e and p_e are the total energy and momentum of the β , W_0 its maximum total energy, A_0 and C_0 are factors containing all the matrix elements, C_0 is defined in Appendix A, and, for $0^+ \rightarrow 1^+$ transitions, such as the one discussed in this paper, $A_0 = 0$. $F_0 L_0$ takes into account the Coulomb interaction between the β 's and the nucleus, and $C(W_e)$ is called the "shape factor." It is this $C(W_e)$ part of the energy dependence of the spectrum that we want to address in this work. In a typical allowed Gamow-Teller (GT)—axial—matrix element and its interference with the weak-magnetism (WM)—vector—matrix element:

$$\langle \sigma \rangle^2 C(W_e) \approx \langle \sigma \rangle^2 \pm \frac{4}{3M} \langle \sigma \rangle \langle \text{WM} \rangle (W_e - W_0/2) \quad (2)$$

where M stands for the nucleon mass. Thus, by measuring the shape of the β spectrum, one can extract the $\langle \text{WM} \rangle$ matrix element. A measurement of this kind in the $A = 12$ system was proposed by Gell-Mann [3] to check on the conservation of the vector current (CVC) hypothesis [4] according to which the operator WM in the β decay of ^{12}B and ^{12}N should be equal to the $M1$ operator that determines the width of the electromagnetic transition from the isobaric analog state:

$$\langle M1 \rangle^2 = 6 \frac{\Gamma_\gamma}{\alpha} \frac{M^2}{E_\gamma^3}. \quad (3)$$

Adding the condition of charge symmetry one concludes that $\langle \text{WM} \rangle = \langle M1 \rangle$. Many authors [5–7] have undertaken the difficult task of measuring the shape of the $A = 12$ β -decay spectra. Table I presents the results of these efforts, which show

discrepancies that go beyond their statistical errors, and leave the impression that each experiment may be affected by systematic problems which are hard to estimate. What makes these measurements particularly hard is the fact that the slope corresponding to Eq. (2) is only about $5 \times 10^{-3} \text{ MeV}^{-1}$.

In what follows we will address the problems of calculating the shape of the β spectra in the $A = 14$ system and we will analyze its potential for being used to test the CVC hypothesis.

II. CVC AND THE IMPULSE APPROXIMATION

The β decay of ^{14}C is famous for its extremely hindered transition rate [8] due to a particularly small GT matrix element which has been shown to be possible only if a tensor force is at work [9]. This implies that the spectrum slope expected according to Eq. (2) should be much larger than the one expected in the $A = 12$ system. In the approximation described by Eq. (2) the two matrix elements can be fixed by requiring $\langle \sigma \rangle$ to give the correct half-life, and $\langle \text{WM} \rangle$ to be equal to $\langle M1 \rangle$ in the analog electromagnetic transition, according to CVC plus charge independence of the nuclear interactions. One can approximately separate these two requirements because the $\langle \sigma \rangle \langle \text{WM} \rangle$ term vanishes to order α when integrating over the whole β spectrum [10]. Calaprice and Holstein [11] calculated the expected shape factors in a series of nuclei using Eq. (2) and obtained

$$C(W_e) \approx 1 \pm 0.38(0.05) W_e \quad \text{for } ^{14}\text{C}(^{14}\text{O}) \quad (4)$$

with W_e in MeV. This amplification of a factor ≈ 50 with respect to the $A = 12$ system has some drawbacks. In our case

TABLE I. Results of measurements of shape factors in the $A = 12$ system.

Reference	a_- (% MeV^{-1})	a_+ (% MeV^{-1})
M.-K. [5]	$+1.82 \pm 0.09$	$+0.60 \pm 0.08$
Wu [6]	$+0.41 \pm 0.1$	-0.45 ± 0.09
Ka. [7]	$+0.91 \pm 0.11$	-0.07 ± 0.09

the GT matrix element is so small ($\approx 2 \times 10^{-3}$ for ^{14}C) that other terms not included in Eq. (2) become relatively important and have to be taken into account. In fact, Calaprice and Holstein noticed a discrepancy of about a factor of 2 between the prediction of Eq. (4) and a measurement of the shape factor of ^{14}O [12] and suggested that this discrepancy could be due to an enhancement of electromagnetic effects.

CVC relates the operators for the $M1$ electromagnetic transition and the isobaric analog vector part of the weak current, but in order to equate $\langle M1 \rangle$ with $\langle \text{WM} \rangle$ one needs to demand the wave functions in the initial state (^{14}C , $^{14}\text{N}^*$, and ^{14}O) to be equal. The electromagnetic interaction breaks charge independence but these effects are usually very small. However, in the $A = 14$ case there seems to be a special cancellation at work which makes the GT matrix element very small. This cancellation effect is sensitive to changes in the wave functions and to renormalizations of the operator as is evidenced by the large ft asymmetry: $B(\text{GT})(^{14}\text{O}) \approx 59 B(\text{GT})(^{14}\text{C})$.

We note another singularity of the $A = 14$ system regarding CVC: the anomalous magnetic moment contribution to the magnetism is expected to be negligible, so there is no anomalous enhancement of the weak magnetism, but CVC still prescribes the nonrenormalizability of this operator.

We will now turn to the calculation of the matrix elements.

III. PREVIOUS WORK IN THE $A = 14$ SYSTEM

Recently, Genz *et al.* [13] presented calculations of the shape of the β spectra in the $A = 14$ system, using $0\hbar\omega$ wave functions (i.e., two- $0p$ -shell holes in ^{16}O). General LS -coupled wave functions have the form

$$|^{14}\text{N}\rangle = \alpha|^3S_1\rangle + \beta|^1P_1\rangle + \gamma|^3D_1\rangle, \quad (5)$$

$$|^{14}\text{C}\rangle = \xi_-|^1S_0\rangle + \eta_-|^3P_0\rangle, \quad (6)$$

$$|^{14}\text{N}^*\rangle = \xi_0|^1S_0\rangle + \eta_0|^3P_0\rangle, \quad (7)$$

$$|^{14}\text{O}\rangle = \xi_+|^1S_0\rangle + \eta_+|^3P_0\rangle. \quad (8)$$

Genz *et al.* fixed the coefficients by requiring agreement with the following data set: (1) elastic and inelastic e^- scattering on ^{14}N ; (2) the $\log ft$'s measured for the β^\pm decays; (3) the shape factor of ^{14}C measured by Sonntag *et al.* [14], and of ^{14}O measured by Sidhu and Gerhart [12]. In order to make these comparisons they used the formalism of Behrens and Bühring [2] and the impulse approximation to calculate matrix elements. The formalism accounts in a consistent way for the Coulomb interaction of β 's with the nucleus, and the expressions include contributions of all matrix elements to the spectrum shape. Expressions from an equivalent formalism by Holstein [15] do not include all terms containing products of induced weak-current matrix elements. The latter is particularly important in the present case, because, as we mentioned earlier, the fact that the GT matrix element is so small makes it necessary to include all the usually neglected terms that contribute to the shape of the β spectra. We shall also use the formalism of Behrens and Bühring [2].

Genz *et al.* noted that, assuming $0p$ oscillator wave functions, the matrix elements necessary for the calculation of the β -decay observables appear only in the following combinations:

$$V_1 = \frac{M_{101}^0}{\sqrt{3}}, \quad (9)$$

$$V_2 = \left(\frac{R}{b}\right)^2 \frac{1}{5} \sqrt{\frac{2}{3}} M_{121}^0, \quad (10)$$

$$V_3 = -\frac{MR}{3} M_{111}^0 - \frac{M_{101}^0}{\sqrt{6}}, \quad (11)$$

$$V_4 = \frac{MR}{3} M_{110}^0. \quad (12)$$

Here V_1 corresponds to the $\langle \sigma \rangle$ matrix element, V_3 contains the orbital part of either the $M1$ transition or the weak-magnetism matrix elements, and V_4 contains the contributions from the first-class induced tensor—see Appendix B for a list of correspondences to Holstein's matrix elements.

In Cartesian notation, these matrix elements are

$$M_{101}^0 = \int \sigma, \quad (13)$$

$$M_{121}^0 = -\frac{3}{\sqrt{2}} \int \frac{(\sigma r) \mathbf{r} - (1/3) \sigma r^2}{R^2}, \quad (14)$$

$$M_{111}^0 = -\sqrt{\frac{3}{2}} \int \frac{\alpha \times \mathbf{r}}{R}, \quad (15)$$

$$M_{110}^0 = \sqrt{3} \int \gamma_5 i \frac{\mathbf{r}}{R}. \quad (16)$$

We note that the M coefficients defined by Behrens and Bühring do not contain contributions from induced currents. The induced currents are correctly accounted for in the definition of the F terms defined in Appendix A, which are used to calculate the measurable quantities.

Genz *et al.* showed that none of the previous " $0\hbar\omega$ " calculations could account for all experimental observations in the $A = 14$ system. They carried out a calculation releasing the constraint of charge independence and obtained better agreement with experiment. The values they obtain for the four matrix elements are shown in Table II. The resulting values for the shape factors are

$$C(W_e) \approx 1 - 0.67(0.10)W_e \quad \text{for } ^{14}\text{C}(^{14}\text{O}). \quad (17)$$

We note that Genz *et al.*'s wave functions show too strong a charge dependence. For example, a simple overlap of the $^{14}\text{O}(0^+)$ and $^{14}\text{N}(0^+)$ wave functions differs about 1.3% from unity, while this difference is supposed to be at least a factor of 5 smaller [16]. In addition, Genz *et al.*'s wave function for the 0^+ level has much too high of a probability for the $p_{3/2}^-$ configuration compared to the $p_{1/2}^-$ configuration—

TABLE II. Results for V coefficients using different wave functions.

Reference	V_1	V_2	V_3	V_4
Genz [13] (^{14}C)	0.002	-0.364	-0.524	0.006
Genz [13] (^{14}N)	0.085	-0.477	-0.585	-0.002
Genz [13] (^{14}O)	-0.006	-0.353	-0.518	0.006
C and K (POT) (Genz) ^{a,b}	0.220	-0.905	-0.489	0.091
C and K (BME) (Genz) ^a	0.071	-0.916	-0.452	0.144
C and K (POT) (This work) ^a	0.218	-0.904	-0.488	-0.092
C and K (BME) (This work) ^a	0.072	-0.915	-0.453	-0.144
WBT [17]	-0.084	-0.911	-0.410	-0.223
WBTM [17]	0.063	-0.923	-0.472	-0.168
WBTM2 [17]	0.063	-0.375	-0.472	-0.168

^aWe obtain values of V_4 of opposite sign to those published by Genz *et al.*

^bC and K (POT) and (BME) are defined in Ref. [18].

the ratio of squared amplitudes is 3.5 for ^{14}O whereas experiment shows this ratio should be about 0.2.

IV. OUR SHELL-MODEL WAVE FUNCTIONS

We now turn to discuss our shell-model wave functions and the expected effects of charge-symmetry breaking.

A. Wave functions

The initial wave functions were obtained in the $0p$ -shell-model space with the $0p$ -shell part of the Warburton-Brown (WBT) Hamiltonian [17] (the interaction labeled PWBT in Table X of Ref. [17]). This interaction was determined from a least-squares fit of 51 $0p$ -shell binding energies together with 165 $0p$ - $0d1s$ cross-shell binding energies. The rms deviation for the 51 $0p$ -shell data (Table III of [1]) was 378 keV. The $0p$ -shell part of the WBT interaction can be considered a refinement of the original Cohen-Kurath [18] formulation of the interaction.

We are interested in further refining the wave function for the $0^+ T=1$ and $1^+ T=0$ states in $A=14$. We do this in two ways. First we note that the $M1$ and GT transition strengths to the lowest 1^+ state are very small compared to the strengths of the transition to the second 1^+ state at $E_x=3.95$ MeV. Thus any small mixing between these two 1^+ states in the model will have a large effect on the weak transition rate. This small mixing could originate from non- $0p$ -shell parts of the wave functions as well as from effective three-body forces not present in the calculation. We deter-

mine the mixing by reproducing the experimental $0^+ T=1$ to $1^+ T=0 B(M1)$ value of $0.017\mu_N^2$ [19]. The mixed wave functions are

$$|1^+\text{low}\rangle = 0.993|1^+(1)\rangle + 0.118|1^+(2)\rangle \quad (18)$$

and

$$|1^+\text{high}\rangle = -0.118|1^+(1)\rangle + 0.993|1^+(2)\rangle \quad (19)$$

where (1) and (2) refer to the first and second WBT model states. The $B(M1)$ values before and after mixing are $0.113\mu_N^2$ and $0.017\mu_N^2$, respectively. We will refer to these mixed wave functions as WBTM. In perturbation theory this mixing results from an off-diagonal interaction of about $0.118 \times (3.9\text{MeV}) = 460$ keV which is not inconsistent with the 378 keV rms deviation found for the energy levels. The $0^+ T=1(^{14}\text{C})$ to $1^+ T=0(^{14}\text{N})$ GT matrix element changes from -0.181 to 0.136 . In order to compare these to ft values one needs to include contributions from other matrix elements and we shall do this later. We could also mix the wave functions to give *zero* for the GT matrix element with the result

$$|1^+\text{low}\rangle = 0.9977|1^+(1)\rangle + 0.0678|1^+(2)\rangle \quad (20)$$

and

$$|1^+\text{high}\rangle = -0.0678|1^+(1)\rangle + 0.9977|1^+(2)\rangle. \quad (21)$$

This mix gives $B(M1) = 0.047\mu_N^2$. One should not expect any purely nucleonic wave functions to reproduce both $B(M1)$ and $B(GT)$ exactly because the mesonic exchange

TABLE III. Expected variations on matrix elements V 's due to INC effects: isospin mixing.

	WBT OB			WBT OB M		
	^{14}C	^{14}N	^{14}O	^{14}C	^{14}N	^{14}O
V_1	-0.0605	-0.0642	-0.0647	0.0025	-0.0014	-0.0020
V_2	-0.9196	-0.9142	-0.9106	-0.9268	-0.9196	-0.9178
V_3	-0.4230	-0.4194	-0.4179	-0.4515	-0.4472	-0.4452
V_4	-0.2276	-0.2177	-0.2111	-0.2029	-0.1947	-0.1881
$(\mu_p - \mu_n)V_1 / \sqrt{2} + V_3^a$	-0.6241	-0.6328	-0.6329	-0.4432	-0.4518	-0.4518

^a“Magnetic” matrix element: proportional to the $M1$ matrix element in the γ decay, and to the WM matrix element in the β decay.

current corrections are different for the vector ($M1$) and axial vector (GT) decay [20]. However, a quantitative evaluation of the exchange current effects for these weak $M1$ and GT matrix element is probably not reliable. Given the general observation that $M1$ transitions in light nuclei are close to the “free-nucleon” calculations while the GT transitions are systematically hindered [20], we have chosen the WBTM solution for the mixing. The very weak GT matrix element will be fine-tuned later by using the experimental $\log_{10}ft$ value.

Secondly, we explicitly consider the effect of $2\hbar\omega$ admixtures into the $0\hbar\omega$ $0p$ -shell wave function. It is technically straightforward to carry out calculations which include $2\hbar\omega$ and even $4\hbar\omega$ admixtures [21]. However, such calculations are not fully appropriate because the $2\hbar\omega$ and $4\hbar\omega$ admixtures will effectively modify the $0p$ -shell part of the WBT interaction (which was obtained under the assumption of pure $0\hbar\omega$ configurations). The task of redetermining the appropriate effective interaction to be used in the mixed space has not yet been carried out. Thus we consider the $2\hbar\omega$ admixture in perturbation theory where its effect on the transition can be isolated from its effect on the interaction. The perturbed wave function has the general form

$$a|0\hbar\omega\rangle + b|1p1h;2\hbar\omega\rangle, \quad (22)$$

where $|0\hbar\omega\rangle$ represents the WBTM $0p$ -shell wave functions, and $1p1h$ indicates a one-particle one-hole excitation relative to the $0p$ -shell configuration. This includes the excitation of $0s$ to $0d1s$ and $0p$ to $0f1p$. First-order perturbation theory accounts for terms of order b/a neglecting the small $(b/a)^2$ contributions. The $2p2h;2\hbar\omega$ admixtures do not affect the transition matrix element to first order because the one-body operator cannot connect $0p0h$ (the $0p$ wave function) with $2p2h;2\hbar\omega$. The effect of $1p1h$ and $2p2h;2\hbar\omega$ on the $0p$ -shell effective Hamiltonian is implicitly taken into account by the WBT interaction and its modification to WBTM. Such perturbation calculations for the $E2$ matrix elements $\langle r^2 Y^2 \rangle$, are well established [22,23] and show that $1p1h;2\hbar\omega$ admixtures (the giant quadrupole resonance) greatly enhance the $E2$ transition strength. For our perturbation calculations we use the δ -function interaction of Ref. [22]. We find that these $1p1h;2\hbar\omega$ admixtures have an important effect on the shape of the isovector $M1$ form factors. The result for the ^{12}C $M1$ transition is to bring the first maximum and first minimum in the form factor into much better agreement with experiment compared to a pure $0p$ calculation [24]. The effect on the ^{14}N $M1$ transition is to quench the form factor at its peak. When $B(M1, q)$ is plotted as in Fig. 1 the effect of $2\hbar\omega$ admixtures is to reduce the slope. We will come back to discussing this figure in Sec. V. The $2\hbar\omega$ admixtures have no effect on the $B(M1)$ and $B(\text{GT})$ values because the matrix element terms proportional to ab vanish. The results in which WBTM are modified by the addition of $2\hbar\omega$ admixtures are referred to as WBTM2.

We have also examined other properties of the ^{14}N ground state. The transverse elastic electron scattering data are well reproduced with WBTM and WBTM2. The calculated magnetic moments are $0.340\mu_N$ and $0.312\mu_N$ for WBT and WBTM (and WBTM2), respectively. Using the relations $\mu = g_l \langle L_z \rangle + g_s \langle S_z \rangle$ and $J = \langle L_z \rangle + \langle S_z \rangle$, where the expecta-

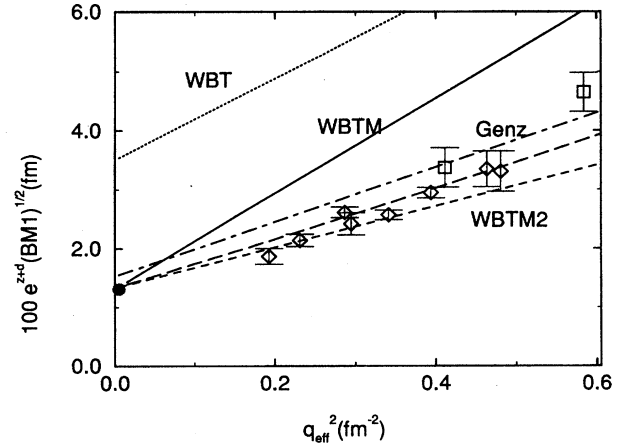


FIG. 1. Comparison of measurements of inelastic scattering cross section to our fits. We have plotted the points using q_{eff} as defined in the text. The factor $\exp(-d)$ represents the center-of-mass and single-nucleon-form-factor corrections. The data are from Huffman *et al.* [27] (squares), Ensslin *et al.* [28] (circles), and Genz *et al.* [13] (diamonds). The point at $q^2=0$ corresponds to a width for the $M1$ transition of 6.7 ± 0.3 meV. The curves correspond to the values of the V matrix elements shown in Table II, except for WBTM2, for which we have made plots both including (long dashed) and not including (short dashed) the q^4 contributions from “ $2\hbar\omega$ ” admixtures.

tion values are taken in the $M=J$ substate and where $g_l=0.5$ and $g_s=0.880$ are the isoscalar g factors, the isoscalar moment can be used to obtain the $\langle S_z \rangle$ expectation value [25]. The results for the ^{14}N ground state are -0.25 , -0.42 , and -0.49 for experiment, WBT, and WBTM, respectively. One observes a quenching of the $\langle S_z \rangle$ value which is consistent with that for the $A=15$, $T=1/2$ ground state isoscalar moment (the average of the mirror moments) which is -0.084 and -0.166 for experiment and $0p_{1/2}$, respectively—the $0p$ -shell model for $A=15$, $T=1/2$ is a pure $0p_{1/2}$ single-particle state and this should be compared on the same footing with the WBTM (or WBT) result for $A=14$. The particular higher-order mixing which affects these isoscalar observables is not relevant for the isovector quantities which are needed in the β decay. The calculated quadrupole moments are 1.19 , 0.92 , and $1.57 e \text{ fm}^2$ for WBT, WBTM, and WBTM2, respectively. The first two are obtained with free-nucleon effective charges and the last one includes the standard effective changes of $e_p=1.35$ and $e_n=0.35$ which result from the $2\hbar\omega$ admixtures [26]. The WBTM2 value of Q agrees with the experimental Q moment of $1.6 e \text{ fm}^2$.

Regarding the spectroscopic factors, the values calculated with the WBT wave functions for ^{15}N to ^{14}N are $C^2S(p_{3/2}, J_f^\pi=1^+) = 0.146$, $C^2S(p_{1/2}, J_f^\pi=1^+) = 1.22$, and $C^2S(p_{1/2}, J_f^\pi=0^+) = 0.45$, in very good agreement with experimental values of 0.10 ± 0.08 , 1.24 ± 0.09 , and 0.47 ± 0.01 , respectively, obtained from the $^{15}\text{N}(d,t)^{14}\text{N}$ reaction [27]. In contrast, Genz *et al.* obtain 0.187 for $C^2S(p_{1/2}, J_f^\pi=0^+)$. The effect of mixing the 1^+ states by the amount given by Eq. (18) has a negligible effect on these spectroscopic factors.

B. Effects of charge-symmetry breaking

The effects of charge-symmetry breaking are traditionally broken down into two corrections, (1) the “isospin mixing” correction δ_{IM} which takes into account the change in the model-space wave functions due to the presence of Coulomb and isospin nonconserving (INC) nuclear interactions and (2) the “radial overlap” correction δ_{RO} which takes into account the difference between the proton and neutron radial wave functions between the initial and final states. Both corrections are due to INC interactions (Coulomb and nuclear) but (1) takes into account mixing inside the $0p$ model space and (2) takes into account mixing beyond the $0p$ model space. In Ref. [28] these INC effects were calculated for the ^{14}O Fermi β decay and we will use the same procedures here.

We first consider the IM correction by adding onto the isospin conserving WBT interaction the isospin nonconserving (INC) interaction of Ormand and Brown [28]. This INC interaction is made up of Coulomb, charge-asymmetric, and charge-dependent components whose strengths were obtained from the displacement energies observed for the analog states in the $0p$ shell. The results for WBTOB are given in Table III.

There is a small shift in the values from WBT due the fact that the Coulomb interaction contains a small isospin conserving (isoscalar) part which adds to the WBT interaction. In addition there is now some dependence on T_z due to a change in the 0^+ wave functions. The $(p_{1/2})^{-2}, (p_{3/2})^{-2}$ probabilities for ^{14}O , ^{14}N , and ^{14}C are (0.899, 0.101), (0.906, 0.095), and (0.918, 0.081), respectively.

The overlap of the ^{14}O and ^{14}N configurations gives a correction of less than 0.01% for the Fermi matrix element and is consistent with the results given in Ref. [28]. We note again that the correction of 1.3% obtained with Genz *et al.*'s wave functions is unrealistic—the total mismatch correction expected from universality and unitarity [16] is about 0.5% percent, and is expected to be dominated by the charge dependence of the nucleonic binding energies, and not by the configuration mixing for which Genz *et al.*'s wave functions yield 1.3%.

In order to see to what extent the variations in the extremely forbidden GT matrix elements can be accounted for, we again remix the ^{14}N 1^+ wave functions in order to get an arbitrarily small value for ^{14}C . The mix this time is

$$|1^+ \text{low}\rangle = 0.9987|1\rangle + 0.05097|2\rangle. \quad (23)$$

The results for WBTOBM are given in Table III. We observe that the V_1 matrix element can vary so that $V_1(\beta^-)/V_1(\beta^+) \approx -1$. This is very different than the square root of the ratio of $B(\text{GT})$'s which is about 7. However, as we pointed out before, given the high suppression of the GT matrix element one has to take into account other terms in calculating the ft values. We will show later that a ratio of the $\langle\sigma\rangle$ matrix elements of ≈ -4 would yield a ratio of $B(\text{GT})$'s in agreement with experiment. We speculate that the difference between our prediction and measurement is due to further modifications due to the renormalization of the axial operators. However, one should keep in mind that this large relative asymmetry in the GT matrix element implies variations of about 2% in the “magnetic” matrix element. We will come back to this point later. Other quantities also

TABLE IV. Expected variations on matrix elements V 's due to INC effects: radial overlaps.

	^{14}C	^{14}N	^{14}O
V_1	-0.0035	-0.0015	-0.0009
V_2	-1.1080	-1.1061	-1.0963
V_3	-0.4287	-0.4471	-0.4462
V_4	-0.2029	-0.1947	-0.1881
$(\mu_p - \mu_n)V_1/\sqrt{2} + V_3$ ^a	-0.4403	-0.4521	-0.4492

^a“Magnetic” matrix element: proportional to the $M1$ matrix element in the γ decay, and to the WM matrix element in the β decay.

exhibit some T_z dependence but the change is small compared to the larger variation found, for example, from the remixing of the 1^+ states.

We consider the radial overlap correction by redoing the WBTOBM calculation, replacing the harmonic-oscillator radial wave functions with those obtained from the SGII Skyrme Hartree-Fock calculation [28]. The results are shown in Table IV. The results for ^{14}O and ^{14}C use the overlaps obtained with the proton radial wave function on one side and the neutron radial wave function on the other side of the matrix elements, while the results for ^{14}N use the overlaps with the same radial wave functions on both sides.

We note some increase (relative to the harmonic-oscillator results) for the V_2 matrix element which depends upon the r^2 radial matrix element. However, the change is relatively small compared to that obtained from the $2\hbar\omega$ core polarization. There are further changes in the V_1 matrix element which are again consistent with experiment. The radial overlap effect on V_3 and V_4 is small.

V. FINE ADJUSTMENTS OF MATRIX ELEMENTS TO FIT DATA

We will now discuss the modifications in the matrix elements which are needed to obtain a better fit of experimental data. Our approach is to try to fix only the matrix elements needed for the calculation of the shape factor by a minimal adjustment which is required to obtain agreement with experimental data.

We will use the WBTM2 wave functions discussed above to calculate the value of V_2 and V_4 . The calculations of the matrix elements necessary for β decay were performed in the formalism of Holstein [15], which we show in Table V, and then translated according to the recipes shown in Appendix B. We note (see also Table II) that our value for the relative sign of d_1 and b differs from that obtained by Genz. We have checked our sign convention against three previous calculations for other mass systems [29–31]. We also calculated the V matrix elements in LS coupling and obtained agreement with Genz *et al.* except in the sign of V_4 . In our calculation we included a $(-)^{L+S+1}$ sign change due to the translation from “particles” to “holes.”

Following, we fix $V_1(\gamma)$, $V_1^A(\beta^\mp)$, and V_3 requiring agreement with the width of the $M1$ transition, the inelastic scattering $^{14}\text{N}(e, e')$ data, and the β^\mp log ft . We use the following relations.

(1) The width of the $M1$ transition is related to the vector form factor by

TABLE V. Results of the calculation of $A = 14$ matrix elements.

Definition ^a	WBT	WBTM	WBTM2
$c_1^H = \lambda M_{GT}$	-1.8110^{-1}	1.3610^{-1}	1.3610^{-1}
$c_2^H = \frac{\lambda}{6} [M_{\sigma r^2} + (1/\sqrt{10})M_{1y}]$	7.47×10^{-1}	1.14	5.99×10^{-1}
$b^H = \hat{A}(g_M M_{GT} + g_V M_L)$	-2.36×10^1	-9.04	-9.04
$d_l^H = \lambda A M_{\sigma L}$	1.35×10^1	1.02×10^1	1.02×10^1
$h^H = -(2/\sqrt{10})(MA)^2 \lambda M_{1y} / (\hbar c)^2 - A^2 g_P M_{GT}$	-5.18×10^4	-4.65×10^4	-1.61×10^4
$h_1^H = -(2/\sqrt{10})(MA)^2 \lambda M_{1y} / (\hbar c)^2$	-5.05×10^4	-5.12×10^4	-2.08×10^4

^aWe use $\lambda = 1.25$; $g_M = 4.7$; $g_P = -(2M_p/m_\pi)^2 \lambda = -222$, related to f_p used with Behrens and Janecke notation by $f_p = g_P/2M_p$; $M_p = 938.9$ MeV and $M = 931.5$ MeV.

$${}^v F_{111}^0 = \sqrt{9\Gamma_\gamma I(\alpha R^2 E_\gamma^3)} \quad (24)$$

where we use $\Gamma_\gamma = 6.7 \pm 0.3$ meV, from Ref. [32]. Taking into account the third equation in Appendix A, this equation translates to

$$\left| \frac{(\mu_p - \mu_n)}{\sqrt{2}} V_1(\gamma) + V_3 \right| = 0.256 \pm 0.006. \quad (25)$$

(2) The inelastic scattering cross section is proportional to [2]

$$\sqrt{B(M1, q)} = \frac{R}{4\sqrt{3}\pi} {}^v F_{111}(\mathbf{q}^2) \quad (26)$$

where R is the nuclear radius and

$${}^v F_{111}(\mathbf{q}^2) = \frac{3}{MR} \left(-(\mu_p - \mu_n) V_1(\gamma) / \sqrt{2} - V_3 + (\mu_p - \mu_n) \times [V_1(\gamma) - V_2] \frac{\sqrt{2}}{3} z \right) \exp(-z-d) \quad (27)$$

is the form factor [33], and $z = (qb/2)^2$, with the oscillator parameter $b = 1.7$ fm; the term $\exp(-d)$ accounts for the center-of-mass and single-nucleon-form-factor corrections, with $d = q^2(a_p^2 - b^2/A)/4$, and $a_p^2 = 0.43$ fm² [34,35].

The first term gives the $M1$ width that we used in the previous item, and the term dependent on q^2 gives the condition

$$|-V_1(\gamma) + V_2| = 0.422 \pm 0.006 \quad (28)$$

where the expression contained within the absolute value bars has to have the same sign as the expression inside the absolute bars of Eq. (25). This sign arrangement is the only way of getting agreement with the width of the $M1$ transition and the inelastic scattering data simultaneously as can be seen from Eq. (27). The numbers and errors in the right side of Eqs. (25) and (28) were obtained from a χ^2 fit to the inelastic scattering plus $B(M1)$ data shown in Fig. 1, with a correction to the number in Eq. (28) that we explain below. We also show the predictions of the WBT, WBTM, and WBTM2 wave functions. We translated the momentum transfer into q_{eff} using the following equation:

$$q_{\text{eff}} = q \left(1 + \frac{3\sqrt{3}}{2\sqrt{5}} \frac{Z e^2}{\sqrt{\langle r^2 \rangle} E_0} \right) \quad (29)$$

to account for the distortion of the electron wave by the Coulomb field of the nucleus [36]. Here E_0 indicates the beam energy and $\langle r^2 \rangle$ the mean square radius. Also, in Fig. 1 we have divided the experimental data by the center-of-mass and single-nucleon-form-factor corrections. Although Eq. (27) is complete in a $0p$ -shell calculation, there are additional contributions from outside the $0p$ shell, that come to order q^4 and become important as q^2 gets larger. For that reason, we have only used electron scattering data with $q^2 \leq 0.6$ fm⁻². In Fig. 2 we show the electron scattering data up to higher momentum transfers. We plot the WBTM2 results both with and without the q^4 contributions. Because these q^4 contributions do affect the slope even at $q^2 \leq 0.6$ fm⁻² by about 15%, as can be seen in Fig. 1, our number in the right hand side of Eq. (28) has been decreased from the best fit of -0.497 ± 0.007 by 15%.

(3) The ft^- value is given by

$$ft = \frac{6170}{C_0^2 \bar{C}(W_e)}. \quad (30)$$

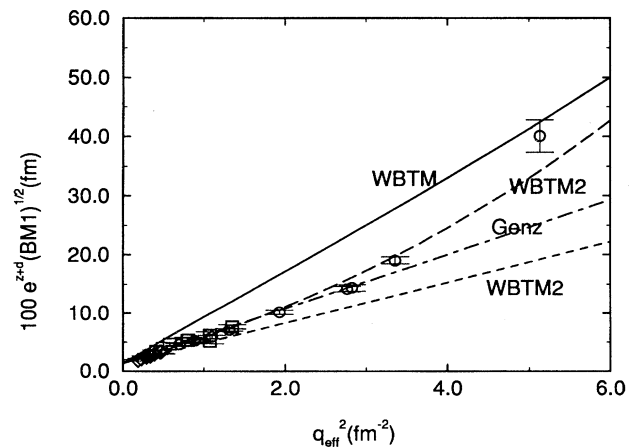


FIG. 2. Same as Fig. 1, but including larger values of q to show the effects of q^4 contributions.

TABLE VI. Calculated parameters for shape of β spectra with V_2 and V_4 from shell-model calculation; V_1 's and V_3 fitted to reproduce experiment, assuming $V_1^V(\beta^\mp) = V_1^A(\beta^\mp)$.

V_2 and V_4 from	$V_1(\beta^\mp)$	$V_1(\gamma)$	V_2^a	V_3	V_4^a	$\langle \text{WM} \rangle / \langle M1 \rangle$	$\bar{\beta}$ (MeV $^{-1}$) ^b
$^{14}\text{C}(\text{WBTM2})$	0.0016	0.0470	-0.3750	-0.4111	-0.1683	1.5904	-0.497
$^{14}\text{C}(\text{WBT})$	-0.0034	-0.4886	-0.9106	1.3687	-0.2227	-5.3235	-1.176
$^{14}\text{C}(\text{WBTM})$	-0.0033	-0.5012	-0.9232	1.4160	-0.1683	-5.4880	-1.179
$^{14}\text{O}(\text{WBTM2})$	-0.0077	0.0470	-0.3750	-0.4111	-0.1683	1.7121	-0.079
$^{14}\text{O}(\text{WBT})$	0.0063	-0.4886	-0.9106	1.3686	-0.2227	-5.4481	-0.147
$^{14}\text{O}(\text{WBTM})$	0.0063	-0.5012	-0.9232	1.4105	-0.1683	-5.6116	-0.151

^aFrom shell-model calculation.

^bWe calculated the shape factor with the values obtained for a , b , and c , according to the last equation of Appendix A, and then obtained the best straight line that fitted it. This column is the ratio of the slope to the value at zero energy.

C_0 and $C(W_e)$ are given in Appendix A in terms of V_1, V_2, V_3 , and V_4 . We use $\log_{10} ft = 9.04$ for ^{14}C , and $\log_{10} ft = 7.27$ for ^{14}O .

It is important to use the measured $\log ft$ to determine the GT matrix element because, as we mentioned before, small variations in the wave functions produce large changes in it, and consequently in the estimated shape of the β spectra. For example, Genz *et al.*'s wave functions give $\log_{10} ft = 9.48$ vs a measured $\log_{10} ft = 9.04$. Although this discrepancy of a factor of 2.5 in the decay rate does not translate with power 1/2 into the shape factor as one could naively expect from Eq. (2) [37] due to the relative importance of higher-order terms, it does have a 10% effect.

V_1 is the matrix element of the σ operator. The β -decay matrix element depends upon a linear combination of operators some of which originate from vector currents (such as $^V F_{111}$ in Appendix A) and some of which originate from axial currents (such as $^A F_{101}^0$ in Appendix A). The σ operators originating from these two cases are labeled $V_1^V(\beta)$ and $V_1^A(\beta)$, respectively. The conservation of the vector current hypothesis relates $V_1^V(\beta)$ to $V_1(\gamma)$. However, if the operator is axial, there can be renormalization effects from mesonic exchange currents and $V_1^A(\beta)$ is in general not equal to $V_1^V(\beta)$. In view of the high sensitivity of V_1 to small variations in the wave functions, and given the effect of exchange currents, we let V_1 take different values for the axial and vector currents in the β decay. Moreover, because we expect charge symmetry breaking, we should allow the vector V_1 matrix element to have different values in the β^- , γ , and β^+ decays. Assuming charge-symmetry for the matrix elements that do not have a special suppression (V_2, V_3, V_4) we

have a total of eight matrix elements to fit: $V_1^V(\beta^\mp), V_1(\gamma), V_1^A(\beta^\mp), V_2, V_3$, and V_4 . Because we have only six observables, namely, the $\log ft$'s, two observables from electron scattering, and the β^\mp shape factors, we follow two alternative paths.

(1) We assume axial and vector matrix elements to be equal, $V_1^A(\beta^\mp) = V_1^V(\beta^\mp) = V_1(\beta^\mp)$, but let $V_1(\gamma)$ vary independently.

(2) We assume the vector matrix elements to be equal, $V_1^V(\beta^\mp) = V_1(\gamma) = V_1^V$, but let $V_1^A(\beta^\mp)$ vary independently. Our option (1) follows the lines of the work of Genz *et al.* but, knowing the significant modifications that axial currents are subjected to in the nuclear medium and based on our estimates for charge-symmetry breaking from Sec. IV B, we believe our option (2) should be more accurate. For either of the options we have six matrix elements to fit: (1) $V_1(\beta^\mp), V_1(\gamma), V_2, V_3, V_4$; (2) $V_1^V, V_1^A(\beta^\mp), V_2, V_3, V_4$. In both cases we take only the solutions yielding negative slopes for both the β^- and β^+ decays, because experiment indicates this is the case.

A. Calculation assuming $V_1^A(\beta^\mp) = V_1^V(\beta^\mp)$

We now calculate the shape of the β spectra assuming $V_1^A(\beta^\mp) = V_1^V(\beta^\mp)$. We first fix the values of V_2 and V_4 using our shell-model calculation. Next we use Eq. (28) to get the value of $V_1(\gamma)$, and then Eq. (25) to fix the value of V_3 . Finally, we fix the values of $V_1(\beta^\mp)$ that satisfy Eq. (30).

The results are shown in Table VI. The $C(W_e)$ factors do not deviate from a straight line significantly so we have cal-

TABLE VII. Arbitrary values for $V_2; V_4$ from WBTM2; assuming $V_1^V(\beta^\mp) = V_1^A(\beta^\mp)$.

$V_1(\beta^-)$	$V_1(\gamma)$	$V_1(\beta^+)$	V_2^a	V_3	V_4^b	$\bar{\beta}(^{14}\text{C})$	$\bar{\beta}(^{14}\text{O})$
0.0011	-0.0780	-0.0083	-0.5000	0.0042	-0.1683	-0.041	-0.017
0.0013	-0.0280	-0.0080	-0.4500	-0.1619	-0.1683	-0.265	-0.045
0.0015	0.0220	-0.0078	-0.4000	-0.3281	-0.1683	-0.430	-0.069
0.0018	0.0720	-0.0076	-0.3500	-0.4943	-0.1683	-0.556	-0.090
0.0020	0.1220	-0.0073	-0.3000	-0.6605	-0.1683	-0.654	-0.108
0.0022	0.1720	-0.0071	-0.2500	-0.8266	-0.1683	-0.733	-0.124

^aArbitrarily fixed to this value.

^bFrom WBTM2 shell-model calculation.

TABLE VIII. Similar to Table VI, but assuming $V_1^V(\beta^\mp) = V_1(\gamma)$.

V_2 and V_4 from	V_1^A	V_1^V	V_2^a	V_3	V_4^a	$\langle \text{WM} \rangle / \langle M1 \rangle$	$\bar{\beta}$ (MeV $^{-1}$) ^b
^{14}C (WBTM2)	0.0015	0.0470	-0.3750	-0.4111	-0.1683	1.0000	-0.363
^{14}C (WBT)	0.0007	-0.4886	-0.9106	1.3687	-0.2227	1.0000	-0.413
^{14}C (WBTM)	0.0008	-0.5012	-0.9232	1.4106	-0.1683	1.0000	-0.418
^{14}O (WBTM2)	-0.0079	0.0470	-0.3750	-0.4111	-0.1683	1.0000	-0.054
^{14}O (WBT)	-0.0087	-0.4886	-0.9106	1.3687	-0.2227	1.0000	-0.065
^{14}O (WBTM)	-0.0087	-0.5012	-0.9232	1.4106	-0.1683	1.0000	-0.064

^aFrom shell-model calculation.

^bWe calculated the shape factor with the values obtained for a , b , and c , according to the last equation of Appendix A, and then obtained the best straight line that fitted it. This column is the ratio of the slope to the value at zero energy.

culated the values for c and s such that $C(W_e) = c + sW_e$ has the minimum χ^2 deviation from the calculated shape and we give the value $\bar{\beta} = s/c$. In order to give an idea of the model dependence we also present in Table VII the results of taking only V_4 from the shell-model calculations and a variety of arbitrary values for V_2 . The contour plots in Fig. 3 are meant to exhibit the dependence of the ^{14}C shape factor on both V_2 and V_4 . Similar percentual deviations are observed for ^{14}O .

We observe in this case a high sensitivity of the shape factor with respect to V_2 . The reason is that, given a value of V_2 , Eq. (28) determines the value of $V_1(\gamma)$, and Eq. (25) the value of V_3 . In this case the weak-magnetism matrix element grows apart from the electro-magnetic $M1$ matrix element, because there is no direct constraint between these two. This means that a “wrong” value for V_2 will yield wrong values for the shape factors. We have seen in Sec. IV A how sensitive V_2 is to “ $2\hbar\omega$ ” contributions: $V_2 \approx -0.9$ for WBT and WBTM, while $V_2 \approx -0.4$ for WBTM2. In other words, it is clear that using a $0\hbar\omega$ space calculation together with equating the axial and vector $\langle \sigma \rangle$ matrix elements can yield very unreliable results. This is why Genz *et al.* get high values for the shape factors— $\bar{\beta} = -0.67$ MeV $^{-1}$ for ^{14}C , and $\bar{\beta} = -0.10$ MeV $^{-1}$ for ^{14}O , and a value for the ratio $\langle \text{WM} \rangle / \langle M1 \rangle$ of ≈ 1.7 for both the β^+ and β^- decays.

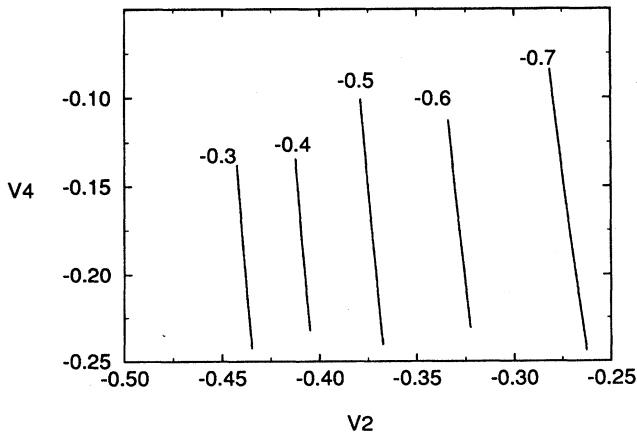


FIG. 3. Contour plots of constant shape factor (in MeV $^{-1}$) for ^{14}C vs V_2 and V_4 assuming $V_1^A(\beta^\mp) = V_1^V(\beta^\mp) \neq V_1(\gamma)$.

Although we observe a large model dependence of the shape factors, the relationship between the β^- and β^+ shape factors is well determined, as we show in Fig. 4, so that, even in this case, there is a clear constraint between the shape factors that originates in CVC.

B. Calculation assuming $V_1(\gamma) = V_1^V(\beta^\mp)$

We note that our charge-symmetry-breaking calculations of Sec. IV B indicate (see Tables III and IV) that one should expect variations in the “magnetic” matrix element, $(\mu_p - \mu_n)V_1 / \sqrt{2} + V_3$, of about 2% due to isospin mixing effects and of about 3% due to radial overlap differences. These are much smaller than the variations we observe in the seventh column of Table VI. So we use now an alternative procedure that guarantees the variations of the vector part of V_1 to be zero: we assume $V_1(\gamma) = V_1^V(\beta^\mp)$. This is not an exact representation of what we believe is happening, but it is more faithful than the previous assumption. We first fix, as we did previously, the values of V_2 and V_4 using our shell-model calculation. Next we use Eq. (28) to get the value of $V_1^V = V_1(\gamma)$, and then Eq. (25) to fix the value of V_3 . Finally, we fix the values of $V_1^A(\beta^\mp)$ that satisfy Eq. 30.

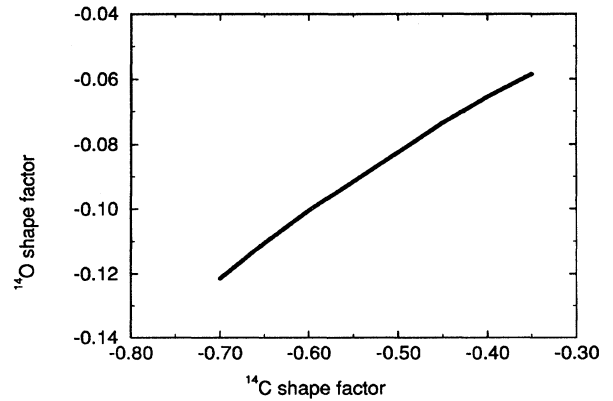


FIG. 4. Value of the shape factor in ^{14}O vs the shape factor in ^{14}C assuming $V_1^A(\beta^\mp) = V_1^V(\beta^\mp) \neq V_1(\gamma)$. Under these conditions we observe a high model dependence of the shape factors, but the relationship between the β^- and β^+ shape factors is well determined.

TABLE IX. Arbitrary values for V_2 ; V_4 from WBTM2; assuming $V_1^V(\beta^\mp) = V_1(\gamma)$.

$V_1^A(\beta^-)$	V_1^V	$V_1^A(\beta^+)$	V_2^a	V_3	V_4^b	$\bar{\beta}(^{14}\text{C})$	$\bar{\beta}(^{14}\text{O})$
0.0013	-0.0780	-0.0080	-0.5000	0.0042	-0.1683	-0.376	-0.056
0.0014	-0.0280	-0.0080	-0.4500	-0.1619	-0.1683	-0.371	-0.055
0.0015	0.0220	-0.0079	-0.4000	-0.3281	-0.1683	-0.366	-0.054
0.0015	0.720	-0.0078	-0.3500	-0.4943	-0.1683	-0.361	-0.053
0.0016	0.1220	-0.0077	-0.3000	-0.6604	-0.1683	-0.356	-0.052
0.0017	0.1720	-0.0077	-0.2500	-0.8266	-0.1683	-0.351	-0.051

^aArbitrarily fixed to this value.

^bFrom WBTM2 shell-model calculation.

Tables VIII and IX are similar to the ones presented in the previous section, but now we observe a much smaller model dependence, because the shape of the β spectra is now fixed by the CVC constraint. This can also be seen, for ^{14}C , in the contour plot of Fig. 5. Similar percentual variations are observed for ^{14}O .

We note that the ratio of the values for V_1^A for β^+ and β^- decays that yields agreement with the measured $\log ft$'s is only about 4 to 5 as opposed to the square root of the ratio of the measured ft values. This is due to the fact that terms other than the GT matrix element contribute significantly to the half-life.

VI. CONCLUSIONS

We have calculated the shape of the β spectra in the $A=14$ system. Our goal was to find out whether second-order and charge-symmetry-breaking effects could somehow be enhanced in this system due to the special cancellation that is observed in the GT matrix element and whether this would imply big deviations from the naive CVC expectations. We have first taken the wave functions obtained with the $0p$ -shell part of the WBT Hamiltonian and added a small mixing between the two lowest 1^+ states to obtain good agreement with the measured width of the $M1$ transition. We have further added “ $2\hbar\omega$ ” contributions and obtained agreement with the $^{14}\text{N}(e, e')$ data without fitting any parameters. These wave functions (WBTM2) cannot account on their

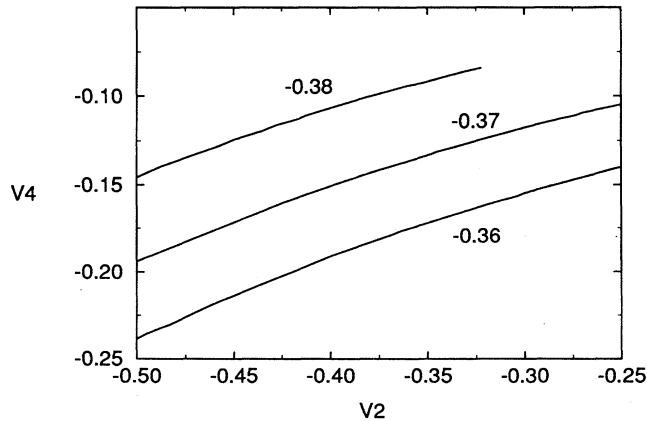


FIG. 5. Contour plots of constant shape factor (in MeV^{-1}) for ^{14}C vs V_2 and V_4 assuming $V_1^V(\beta^\mp) = V_1(\gamma) \neq V_1^A(\beta^\mp)$.

own for the big ft asymmetry observed in the $A=14$ system. The reason is that one has to further take into account possible renormalizations of the axial operators and charge-symmetry-breaking effects. We have done this by independently “fitting” the axial matrix elements so as to obtain agreement with the corresponding $\log ft$ values. Here we have followed two alternative paths. On the one hand, we have shown that assuming the *axial* and *vector* (σ) matrix elements to be equal, as was done previously by Genz *et al.* can lead to a very large charge-symmetry-breaking effect on the magnetic matrix element. The reason is a combination of a lack of enough degrees of freedom in their shell-model calculation, and the fact that the asymmetries in the axial (σ) matrix element translate to asymmetries in the vector magnetic matrix element. Next we have noted that our charge-symmetry-breaking calculations indicate that the $M1$ matrix element is not likely to have differences between the decays of ^{14}O , $^{14}\text{N}^*$, and ^{14}C beyond the 4% level. We note that the “big” observed ft asymmetries imply big asymmetries relative to the size of the GT matrix element, but not with respect to the $M1$ matrix element. So we have performed a different calculation assuming this vector matrix element to have the same value in all three decays. We see the ft asymmetries as arising from a combination of a renormalization of the GT operator that does not affect the vector operator, plus charge-symmetry-breaking effects. *So our main conclusion is that, with respect to the magnetic matrix element, one should not expect very large charge-symmetry-breaking effects in the $A=14$ system.* Our calculation indicates that the shape factors should be $\bar{\beta}(^{14}\text{C}) = -0.37 \pm 0.04$ and $\bar{\beta}(^{14}\text{O}) = -0.055 \pm 0.005$ where the error bars are supposed to give an idea of our rough estimation of model dependence and are dominated by the uncertainty in the charge-symmetry breaking of the vector matrix elements V_1^V and V_3 .

Present data in ^{14}O favor a large-shape-factor solution. Sidhu and Gerhart [12] obtained 30 years ago $\bar{\beta} = -0.110 \pm 0.005 \text{ MeV}^{-1}$. Measurements of the shape factor of ^{14}C are being undertaken presently. Reference [38] finds $\bar{\beta} = -0.45 \pm 0.04 \text{ MeV}^{-1}$. As can be seen from Tables IX or even VII this implies a value for the ^{14}O shape factor in strong disagreement with the measurement of Sidhu and Gerhart [12]. However, the authors of Ref. [38] point out that there could be some systematic problems in this measurement. Data from other experiments are still under progress [39–41]. A new measurement of the ^{14}O shape factor with special attention to possible systematic errors is highly desir-

able. We stress the fact that the present accepted value for the shape factor of ^{14}O cannot be understood simply on the basis of INC effects. Moreover, if it is true, as we are suggesting, that the measurement of Sidhu and Gerhart had some systematic problems, this would affect the value presently accepted for the branch to the 0^+ analog level in ^{14}N , and could significantly change the conclusions extracted from $0^+ \rightarrow 0^+$ transitions regarding universality and unitarity.

In summary, we have calculated the shape factors for the

β decay in the $A = 14$ system and shown that they should be related by CVC at the 10% level.

ACKNOWLEDGMENTS

A.G. thanks Eugene Commins, Ludwig de Braeckeler, Eric Norman, and Stuart Freedman for many illuminating comments; and the Warren Foundation and NSF for support. B.A.B. would like to acknowledge support from NSF Grant No. PHY-94-03666.

APPENDIX A

The form factor coefficients can be written in terms of the V factors presented in Eqs. (9)–(12) as [13]

$${}^A F_{101}^0 = \mp \lambda \sqrt{3} V_1, \quad {}^A F_{121}^0 = \mp \lambda 5 \sqrt{\frac{3}{2}} \left(\frac{b}{R}\right)^2 V_2 \mp \frac{f_p}{R} \sqrt{2} \left(\frac{-15}{2MR}\right) V_1, \quad {}^V F_{111}^0 = -\frac{3}{MR} [(\mu_p - \mu_n) V_1 / \sqrt{2} + V_3],$$

$${}^A F_{110}^0 = \pm \lambda \frac{3}{MR} V_4 \mp \frac{f_p}{R} \left(W_0 R \pm \frac{6}{5} \alpha Z \right) \left(\frac{-3\sqrt{3}}{2MR} \right) V_1, \quad {}^A F_{101}^1 = \mp \lambda \frac{5\sqrt{3}}{2} \left(\frac{b}{R}\right)^2 V_1 \mp \frac{f_p}{R} \left(\frac{-3}{MR}\right) V_1,$$

$${}^A F_{121}^0 \left(\begin{array}{c} I(1,1,1,1) \\ I(2,1,1,1) \end{array} \right) = \mp \lambda \sqrt{6} V_2 \left[\begin{array}{c} 0.823\ 046 \\ 0.789\ 061 \end{array} \right] \mp \frac{f_p}{R} \frac{\sqrt{2}}{3} \left[\sqrt{5} V_2 \left[\begin{array}{c} 0.095\ 968 \\ 0.111\ 351 \end{array} \right] + V_1 \left[\begin{array}{c} -1.525\ 276 \\ -1.413\ 945 \end{array} \right] \right],$$

$${}^V F_{111}^0 [I(1,1,1,1)] = -V_3 0.249\ 939 + \frac{f_M}{R} \sqrt{2} [-V_1 3.515\ 985 + V_2 (-0.379\ 335)] - \frac{1}{\sqrt{2}} \frac{1}{MR} V_1 (-0.823\ 046),$$

$${}^A F_{110}^0 [I(1,1,1,1)] = \pm \lambda V_4 0.249\ 939 \mp \frac{f_p}{R} \frac{1}{\sqrt{3}} \left(W_0 R \pm \frac{6}{5} \alpha Z \right) [\sqrt{5} V_2 0.014\ 577 + V_1 (-0.338\ 465)],$$

$${}^A F_{101}^1 \left(\begin{array}{c} I(1,1,1,1) \\ I(1,2,2,2) \\ I(1,2,2,1) \\ I(1,2,1,1) \end{array} \right) = \mp \lambda \sqrt{3} V_1 \left[\begin{array}{c} 0.823\ 046 \\ 1.174\ 618 \\ 0.883\ 583 \\ -0.060\ 537 \end{array} \right] \mp \frac{1}{3} \frac{f_p}{R} \left[\sqrt{5} V_2 \left[\begin{array}{c} 0.052\ 235 \\ 0.087\ 325 \\ 0.036\ 848 \\ 0.015\ 385 \end{array} \right] + V_1 \left[\begin{array}{c} -0.509\ 881 \\ -0.675\ 066 \\ -0.621\ 254 \\ 0.111\ 352 \end{array} \right] \right].$$

With these one can calculate

$$C_0 = -{}^A F_{101}^0 + \frac{1}{3} W_0 R \left[-\sqrt{\frac{1}{3}} {}^A F_{110}^0 + \sqrt{\frac{2}{3}} {}^V F_{111}^0 \right] + \frac{1}{6} (W_0^2 - 1) R^2 {}^A F_{101}^1 \pm \frac{1}{3} \alpha Z \left\{ -\sqrt{\frac{1}{3}} {}^A F_{110}^0 (1,1,1,1) \right. \\ \left. - \sqrt{\frac{2}{3}} {}^V F_{111}^0 (1,1,1,1) + \frac{1}{9} W_0 R [-{}^A F_{101}^1 (1,1,1,1) + 2\sqrt{2} {}^A F_{121}^0 (1,1,1,1)] \right\} + \frac{1}{6} (\alpha Z)^2 {}^A F_{101}^1 (1,2,2,2),$$

$$C_1 = -\frac{2}{3} \sqrt{\frac{2}{3}} {}^V F_{111}^0 + \frac{2}{27} W_0 R [-5 {}^A F_{101}^1 + \sqrt{2} {}^A F_{121}^0] \pm \frac{1}{3} \alpha Z \left[\frac{1}{9} {}^A F_{101}^1 (1,1,1,1) - \frac{2}{9} \sqrt{2} {}^A F_{121}^0 (1,1,1,1) + {}^A F_{101}^1 (1,2,2,1) \right],$$

$$C_2 = \frac{10}{27} {}^A F_{101}^1 - \frac{2}{27} \sqrt{2} {}^A F_{121}^0,$$

$$D_0 = -\frac{1}{3} \left[\sqrt{\frac{1}{3}} {}^A F_{110}^0 + \sqrt{\frac{2}{3}} {}^V F_{111}^0 \right] + \frac{W_0 R}{27} [-{}^A F_{101}^1 + 2\sqrt{2} {}^A F_{121}^0] \pm \frac{\alpha Z}{6} {}^A F_{101}^1 (1,2,1,1),$$

$$D_1 = \frac{1}{18} \left[\frac{11}{3} {}^A F_{101}^1 - \frac{4}{3} \sqrt{2} {}^A F_{121}^0 \right],$$

$$E_0 = \sqrt{\frac{2}{3}} {}^A F_{110}^0 + \sqrt{\frac{1}{3}} {}^V F_{111}^0 - \frac{1}{5} W_0 R {}^A F_{121}^0 \pm \frac{1}{3} \alpha Z \left[-\frac{2}{3} \sqrt{2} {}^A F_{101}^1(1,1,1,1) - \frac{1}{3} {}^A F_{121}^0(1,1,1,1) \right],$$

$$F_0 = \sqrt{\frac{2}{3}} {}^A F_{110}^0 - \sqrt{\frac{1}{3}} {}^V F_{111}^0 - \frac{1}{9} W_0 R [2 \sqrt{2} {}^A F_{101}^1 + {}^A F_{121}^0] \pm \frac{1}{5} \alpha Z {}^A F_{121}^0(2,1,1,1).$$

These coefficients are now used to calculate the shape parameters:

$$a = R \left[2C_0 C_1 + 2RD_0 D_1 - \frac{2}{9} W_0 R E_0^2 \right] / C_0^2,$$

$$b = -2RD_0 / C_0,$$

$$c = R^2 \left[C_1^2 + 2C_0 C_2 + \frac{1}{9} (E_0^2 + \lambda_2 F_0^2) \right] / C_0^2.$$

The shape factor is

$$C(W_e) = 1 + aW_e + \mu_1 \gamma_1 b / W_e + cW_e^2. \quad (\text{A1})$$

APPENDIX B

We translate the matrix elements from Holstein's notation to the V matrix elements using the results of Table III of Ref. [30]:

$$V_1 = \frac{1}{\sqrt{3}\lambda} c_1^H, \quad (\text{B1})$$

$$V_2 = \frac{1}{2\sqrt{3}\lambda} \left(\frac{\hbar c}{aMA} \right)^2 h_1^H, \quad (\text{B2})$$

$$V_3 = \frac{1}{A\sqrt{6}} b^H - \frac{\mu_p^- \mu_n}{\sqrt{2}} V_1, \quad (\text{B3})$$

$$V_4 = -\frac{1}{2\sqrt{3}\lambda A} d_i^H. \quad (\text{B4})$$

-
- [1] H. Behrens, H. Genz, M. Conze, H. Feldmeier, W. Stock, and A. Richter, *Ann. Phys. (N.Y.)* **115**, 276 (1978).
- [2] H. Behrens and W. Bühring, *Electron Radial Wave Functions and Nuclear Beta-Decay* (Clarendon Press, Oxford, 1982).
- [3] M. Gell-Mann, *Phys. Rev.* **111**, 362 (1958).
- [4] R.P. Feynman and M. Gell-Mann, *Phys. Rev.* **109**, 193 (1957).
- [5] T. Mayer-Kukuk and T.C. Michel, *Phys. Rev.* **127**, 545 (1962).
- [6] C.S. Wu, Y.K. Lee, and L.W. Mo, *Phys. Rev. Lett.* **39**, 72 (1977).
- [7] W. Kaina, V. Soergel, H. Thies, and N. Trost, *Phys. Lett.* **70B**, 411 (1977).
- [8] H.J. Rose, O. Häusser, and E.K. Warburton, *Rev. Mod. Phys.* **40**, 591 (1968).
- [9] D.R. Inglis, *Rev. Mod. Phys.* **25**, 390 (1953).
- [10] S. Weinberg, *Phys. Rev.* **112**, 1375 (1958).
- [11] F.P. Calaprice and B.R. Holstein, *Nucl. Phys.* **A273**, 301 (1976).
- [12] G.S. Sidhu and J.B. Gerhart, *Phys. Rev.* **148**, 1024 (1966).
- [13] H. Genz, G. Kühner, A. Richter, and H. Behrens, *Z. Phys. A* **341**, 9 (1991).
- [14] C. Sonntag, H. Rebel, B. Ribbat, S.K. Tio, and W.R. Gramm, *Lett. Nuovo Cimento* **I4**, 717 (1970).
- [15] B.R. Holstein, *Rev. Mod. Phys.* **46**, 789 (1974).
- [16] D.H. Wilkinson, *Z. Phys. A* **348**, 129 (1994).
- [17] E.K. Warburton and B.A. Brown, *Phys. Rev. C* **46**, 923 (1992).
- [18] S. Cohen and D. Kurath, *Nucl. Phys.* **73**, 1 (1965).
- [19] In order to compare with experimental data we will express $B(M1)$ in units of fm^2 . The relationship between these two systems of units is $B(M1)(\mu_N^2) = (2Mc/\hbar)^2 B(M1)(\text{fm}^2) \approx 90.5 \times B(M1)(\text{fm}^2)$.
- [20] B.A. Brown and B.H. Wildenthal, *Nucl. Phys.* **A474**, 290 (1987).
- [21] E.K. Warburton, B.A. Brown, and D.J. Millener, *Phys. Lett. B* **293**, 7 (1992).
- [22] B.A. Brown, A. Arima and J.B. McGrory, *Nucl. Phys.* **A277**, 77 (1977).
- [23] H. Sagawa and B.A. Brown, *Nucl. Phys.* **A430**, 84 (1984).
- [24] F.P. Brady *et al.*, *Phys. Rev. C* **43**, 2284 (1993); T. Suzuki, H. Hyuga, A. Arima, and K. Yazaki, *Phys. Lett.* **106B**, 19 (1981).
- [25] B.A. Brown and B.H. Wildenthal, *Phys. Rev. C* **28**, 2397 (1983).
- [26] B.A. Brown and B.H. Wildenthal, *Annu. Rev. Nucl. Part. Sci.* **38**, 29 (1988).
- [27] S.K. Saha *et al.*, *Phys. Rev. C* **40**, 39 (1989).
- [28] W.E. Ormand and B.A. Brown, *Nucl. Phys.* **A491**, 1 (1989).
- [29] B.R. Holstein, *Phys. Rev. C* **4**, 741 (1971).
- [30] F.P. Calaprice and D.J. Millener, *Phys. Rev. C* **27**, 1175 (1983).
- [31] F.P. Calaprice, W. Chung, and B.H. Wildenthal, *Phys. Rev. C* **15**, 2178 (1977).

- [32] F. Ajzenberg-Selove, Nucl. Phys. **A523**, 1 (1991).
- [33] There is a printing mistake in the sign of the magnetic moments in Genz *et al.*'s corresponding expression.
- [34] R.L. Huffman, J. Dubach, R.S. Hicks, and M.A. Plum, Phys. Rev. C **35**, 1 (1987).
- [35] N. Ensslin, W. Bertozzi, S. Kowalski, C.P. Sargent, W. Turchinets, C.F. Williamson, S.P. Fivozinsky, J.W. Lightbody, Jr., and S. Penner, Phys. Rev. C **9**, 1705 (1974).
- [36] H. Überall, *Electron Scattering from Complex Nuclei* (Academic Press, New York, 1971).
- [37] We thank Dr. Harald Genz for pointing this out to us.
- [38] F.E. Wietfeldt, E.B. Norman, Y.D. Chan, M.T.F. da Cruz, A. García, E.E. Haller, W.L. Hansen, M.M. Hindi, R.-M. Larimer, K.T. Lesko, P.N. Luke, R.G. Stokstad, B. Sur, and I. Zliten, Phys. Rev. C **52**, 1028 (1995).
- [39] J. Mortara (private communication). This experiment used the apparatus described in J. Mortara *et al.*, Phys. Rev. Lett. **70**, 394 (1993).
- [40] M. Pitt, G.E. Berman, F.P. Calaprice, and N.A. Gorin, Bull. Am. Phys. Soc. **37**, 1286 (1992).
- [41] A. Young (private communication).